Transformations in the Si-O-Ca system: Silicon-calcium via solar energy

Article *in* Solar Energy · February 2019

DOI: 10.1016/j.solener.2019.02.026

6 authors, including:

Daniel Fernández González
University of Oviedo
33 PUBLICATIONS **92** CITATIONS
SEE PROFILE

Janusz Pražuch
AGH University of Science and Technology in Kraków
16 PUBLICATIONS **55** CITATIONS
SEE PROFILE

I. Ruiz-Bustinza
Spanish National Research Council
50 PUBLICATIONS **194** CITATIONS
SEE PROFILE

Carmen González-Gasca
European University of Madrid
13 PUBLICATIONS **66** CITATIONS
SEE PROFILE

Solar Energy 181 (2019) 414–423

Contents lists available at ScienceDirect

Solar Energy

journal homepage: www.elsevier.com/locate/solener

Transformations in the Si-O-Ca system: Silicon-calcium via solar energy

D. Fernández-González[a,*], J. Prazuch[b], I. Ruiz-Bustinza[c], C. González-Gasca[d], J. Piñuela-Noval[a], L.F. Verdeja[a]

[a] Department of Materials Science and Metallurgical Engineering, School of Mines, Energy and Materials, University of Oviedo, Oviedo, Asturias, Spain
[b] Department of Physical Chemistry and Modelling, Faculty of Materials Science and Ceramics, AGH University of Science and Technology, Krakow, Poland
[c] Department of Geological and Mining Engineering, Polytechnic University of Madrid, Madrid, Spain
[d] European University of Madrid-Laureate International Universities, Villaviciosa de Odón, Madrid, Spain

ARTICLE INFO

Keywords:
Concentrated solar energy
Silicon-calcium
Environment
Alloying elements
Solar energy

ABSTRACT

The production of silicon-calcium alloy is energy intensive (> 10,000 kWh/t). This means that energy cost has a relevant influence in the price of the alloy. The utilization of concentrated solar energy in the synthesis of silicon-calcium alloy is proposed in this paper. Metallurgical quality silicon and limestone are used as starting materials (25 wt.%, 50 wt.% and 75 wt.% Si). After a 12 min treatment under power values of around 1 kW and without using special atmosphere, silicon-calcium was detected in all samples, although mixed with the products of reaction ($Ca_3Si_2O_7$, $Ca_{10}O_{25}Si_6$, SiO_2). This last question means that there was not proper separation metal-slag, and it should be improved in future investigations. However, the basic knowledge presented in this paper could be of great interest for an industrial process based on the solar energy. This way, the energy costs could be reduced, the pollutant emissions could be minimized, and the competitiveness of the ferroalloys industry could be increased.

1. Introduction

Solar energy, when properly concentrated, offers a great potential in high temperature applications, and therefore its use in the field of materials has been studied for many years (Fernández-González et al., 2018a). These applications include metallurgy, materials processing (welding and cladding; surface treatments; coatings and surface hardening; and, powder metallurgy), and non-metallic materials (ceramics, fullerenes, carbon nanotubes, and production of lime) (Fernández-González et al., 2018a). In the case of the research group that signs this manuscript, different processes were studied using concentrated solar energy: in the synthesis of calcium aluminates (Fernández-González et al., 2018b), in the indirect reduction of mill scale to produce high quality magnetite (Ruiz-Bustinza et al., 2013), in the direct reduction of iron oxides (laboratory quality reagents, Mochón et al., 2014; Fernández et al., 2015; Fernández-González et al., 2018c; real iron ore sinter, Fernández-González et al., 2018c); and in the treatment of BOF (Basic Oxygen Furnace) slag (Fernández-González et al., 2019).

Silicon-calcium is a strong deoxidizing and desulphurizing element that is used in the production of high-quality steels (Pero-Sanz, 2004; Pero-Sanz et al., 2018). The alloy is used in quantities ranging from 0.5 to 3 kg/ton of steel, with 1–2 kg being the average. The world production of this alloy is very limited because only 150,000 tons of silicon-calcium are produced worldwide. The production of the silicon-calcium is distributed into few plants, for instance, FerroGlobe (one of the biggest producers of ferroalloys) produces approximately 30,000 tons of silicon-calcium alloys in Chateau Feuillet (France) and Mendoza (Argentina). Apart from being a strong deoxidizing and desulphurizing alloy, silicon-calcium alloys allow controlling the shape, size and distribution of the oxides and sulfides inclusions (Sancho et al., 2003). In this way, the fluidity, machinability, ductility and properties of the final product are improved: reduction in the number of inclusions and improvement in their shape, reduction of blowholes during the solidification, improvement in the toughness, etc.

Silicon-calcium alloys are usually produced in submerged arc electric furnaces, which have energy consumptions higher than 10,000 kWh (Robiette, 1973). Mixtures used in the manufacture of silicon-calcium alloys usually comprise quartz/quartzite, lime, fine coke, charcoal and coal. Lime must contain at least 90% CaO because poorly burned lime increases power consumptions, reduces the efficiency of the furnace, implies a non-smooth process and shortens the life of the furnace. Concerning the quality of the different cokes used in ferroalloys industry, their main characteristics can be found in Rodero et al. (2015). Three industrial methods have been developed to produce silicon-

* Corresponding author.
E-mail address: fernandezgdaniel@uniovi.es (D. Fernández-González).

https://doi.org/10.1016/j.solener.2019.02.026
Received 20 November 2018; Received in revised form 7 February 2019; Accepted 12 February 2019

calcium alloys (Robiette, 1973; Tanstad, 2013):

– *Method 1: Simultaneous reduction of calcium and silicon oxides with carbon.*

The raw materials used in this method to produce the silicon-calcium alloy are: lime (> 87% CaO), quartzite (95% SiO_2) and coke. Sulphur quantity in the initial materials must be limited because calcium and sulphur would form CaS during the process. The following chemical reaction describes the process:

$$CaO(s) + 2SiO_2(s) + 5C(s) \rightarrow Ca(l) + 2Si(l) + 5CO(g)$$

The process is governed by the Boudouard mechanism. According to the program HSC5.1 the process becomes favorable above 1700 °C. The reduction is facilitated because of the presence/formation of stable associates close to $CaSi_2$. In this situation, the activity of calcium and silicon is reduced and the recovery of these elements from the oxides is increased. SiC and CaC_2 are formed in the process, and excesses of carbon in the charge must be avoided to minimize the formation of these carbides in the furnace bath. On the contrary, shortage of coke in the charge intensifies the formation of slag from CaO and SiO_2. This leads to losses of raw materials, energy, and problems in the operation of the furnace. A precise dosage of the materials that form the mixture is necessary. Extraction efficiency is normally of 67% for the calcium and of 75% for the silicon (Tanstad, 2013).

– *Method 2: Reduction of calcium oxide with silicon.*

Ferrosilicon is used as reductant agent in this method. If metallic silicon was used, this process would become more expensive due to the price of the metallic silicon (Robiette, 1973). The process can be represented using the following reaction (Tanstad, 2013):

$$4CaO(s) + 6Si(s)(\text{infact, FeSi}) \rightarrow 2Ca(l) + 5Si(l) + 2CaO{\cdot}SiO_2(s)$$

Silicon has higher affinity for the oxygen than the calcium. This question is problematic, and reducing the activity of the calcium is necessary, if the reaction should proceed in the direction of obtaining silicon-calcium alloy. This means that in the final product high silicon and low calcium would be available. As a result, the process has interest in the event of desiring low grades of silicon-calcium (FeSiCa) (< 20% Ca). The industrial practice used to improve the fluidity and, in this way, facilitate the separation melt-slag, is adding fluorspar. The recovery of calcium is low, 20–30%, because there are vaporizations of calcium, while the utilization of ferrosilicon rises to 75–85% (Tanstad, 2013). The quality of the FeSiCa obtained using this method is higher than in the case of the method 1 due to the low sulfur and carbon contents in the alloy.

– *Method 3: Reduction of silicon from quartzite with carbon coming from CaC_2.*

In this case, mixtures used to produce the silicon-calcium alloy include quartzite, calcium carbide and a mixture of coke with charcoal. The process can be described by the reaction:

$$2SiO_2(s) + 2C(s) + CaC_2(s) \rightarrow Ca(l) + 2Si(l) + 4CO(g)$$

From the operational point of view, this process is the least difficult of the three because some calcium is already reduced and there is less CO produced, which tends to reduce the volatilization losses (Robiette, 1973). Other problem of these alloys is their specific gravity because they tend to float on the slag and slag/metal separation is difficult.

The first and the third methods are difficult smelting operations because of the high temperatures (around 1700 °C) required before the process becomes markedly favorable ($\Delta G^\circ < 0$) (Robiette, 1973). Under these conditions there are problems of vaporization, which mean important losses. Thus, the control of the carbon requirements is complicated because excesses of carbon imply the appearance of infusible calcium and silicon carbides, while on the contrary, deficiency of carbon imply fluid calcium silicates resulting in excessive slag losses (Robiette, 1973).

In the experiments described in this manuscript, the utilization of a variation of the *Method 2* is proposed, from now it is called *Method 2.1*, where limestone ($CaCO_3$) instead of lime (CaO) was used, and metallurgical silicon instead of ferrosilicon was employed. The process could be summarized using the following reaction:

$$4CaCO_3(s) + 6Si(s) \rightarrow 2Ca(l) + 5Si(l) + 4CO_2(g) + 2CaO{\cdot}SiO_2(s)$$

Initially, limestone was calcined into lime at around 900 °C (Fernández-González et al., 2018b; Sancho et al., 2003; Ballester et al., 2003), according to the reaction:

$$CaCO_3(s) + heat \rightarrow CO_2(g) + CaO(s)$$

After that, lime is reduced via silicothermic reduction to form calcium, which with the silicon forms the alloy (silicon-calcium):

$$4CaO(s) + 6Si(s)(99\%\text{Si}) \rightarrow 2Ca(l) + 5Si(l) + 2CaO{\cdot}SiO_2(s)$$

Apart from the alloy, silicates of calcium are formed during the process. One of the advantages of the solar process is that could provide a purer alloy because there will not be contamination coming from electrodes. Apart from that, CO_2 emissions could be reduced due to carbon is not used as reductant reagent.

It was previously indicated that *Methods 1* and *3* utilize carbon as reductant reagent, while silicon (or ferrosilicon) is the reductant reagent in the *Method 2*. In the three methods, lime is required to produce calcium for the silicon-calcium alloy. Lime is produced by calcination of the limestone and requires 20–70 kWh of energy per ton of CaO. The calcination of the limestone can be performed in the own process, which was the method used in the experiments presented in this manuscript, or in a separated stage. CO_2 emissions associated to the calcination of the lime are unavoidable, but the emissions associated to the energy (electricity or fossil fuels) used to calcine the limestone might be avoided. The following assumptions were made:

– 0.428 kg CO_2/kWh are emitted in EU28 (average);
– 0.05–0.07 €/kWh for industrials;
– 22.5 €/ton CO_2 is the cost of releasing carbon dioxide in the EU according to the EU Emissions Trading System (with expectative of increasing).

It is possible to check that 8.5–30 kg CO_2/ton of lime might not be emitted only in the production of lime if the generation of heat to produce the lime was taken into account, 1–4.9 €/ton of lime might be saved considering the energy consumption and 0.2–0.7 €/ton lime might be saved only considering the taxes of emitting CO_2. The industrial production of lime using solar energy was studied by Flamant et al. (1980), Imhof (1997), Meier et al. (2004) and Meier et al. (2006). Meier et al. (2004, 2005a, 2006) designed a kiln furnace indirectly heated using a system of rotary tubes. Absorber tubes were heated by means of solar energy and they are responsible of heating the load. Meier et al. (2006) used a 15 kW solar furnace where the experiments required 1.5–2 h to reach stationary conditions and after that the treatment lasted 30 min. Calcination yield of 98.2% and productivities of 64.2 g/min at temperatures of around 1395 K are achieved. Meier et al. (2005b) studied the potential advantages and disadvantages of using concentrated solar energy in the production of lime, and they observed that CO_2 emissions could be reduced by 20% in a state-of-the-art lime plant, and up to 40% in a conventional cement plant. Meier et al. (2005b) calculated the price of the solar lime for a plant of 25 MW, and they observed that the price of the solar lime (128–157 $/ton) was twice that of the conventional lime (in 2004). Thus, producing lime using solar energy in a separated stage seems to mean an increase in the cost of producing the silicon-calcium alloy due to the price of the

lime. That is the reason of using limestone instead of lime in the experiments presented in this manuscript.

The production of silicon-calcium alloy is much more energy intensive than the production of lime. Within 10,000 and 15,000 kWh are required per ton of silicon-calcium alloy depending on the process and operational conditions. For instance, 12,500 kWh per ton of silicon calcium are required in the Method 3 (Robiette, 1973), although producing the calcium carbide would consume approximately 3000 kWh more. As it was previously indicated, silicon-calcium was obtained in this paper using a variation of the *Method 2* that was called *Method 2.1*. Despite this *Method 2.1* would only emit the carbon dioxide produced during the calcination of the limestone, the production of metallurgical silicon requires significant quantities of energy (close to 12,000 kWh/ton silicon) and produces significant emissions of carbon dioxide (5.1 tons CO_2/ton Si (energy) + 4.68 tons CO_2/ton Si (process) (Monses et al., 1998). However, the production of silicon was studied using concentrated solar energy (see Murray et al., 2006; Loutzenhiser et al., 2010; Flamant et al., 2006). In this way, CO_2 emissions could be reduced due to the replacement of the conventional fossil fuels used to heat the industrial furnaces with a clean energy source (solar energy). Considering only the production of the silicon-calcium alloy using one of the methods previously described, the energy required to produce 1 ton of the alloy is within 10,000–15,000 kWh. Making calculations using the assumptions previously indicated, the carbon dioxide emissions associated to the production of silicon-calcium would be in the range 4.3–6.4 ton CO_2/ton silicon-calcium alloy. Regarding the potential reduction of costs (considering the electricity price and the taxes for emitting CO_2): costs of energy, 500–1050 €/ton of silicon-calcium alloy; costs of emitting CO_2, 97–144 €/ton of silicon-calcium alloy. However, to evaluate the real advantages of the solar process (regarding costs), apart from considering the costs of the raw materials, the installation costs should be considered. Flamant et al. (1999) evaluated the installation costs within 1.2–1.8 k€/kW in the range 50–1000 kW. The range of power for the solar furnaces of Flamant et al. (1999) is limited if compare it with that of the industrial furnaces. For instance, the furnace used in Chateau Feuillet to obtain silicon-calcium alloy has a power of 21 MW and produces approximately 18,000 tons of the alloy yearly. Despite the installation costs were not considered because in this paper was studied whether it was possible or not obtaining silicon-calcium using concentrated solar energy, the production of the alloy is energy intensive, and 40–70% of the production costs come from the electricity required by the process. This way, there is a wide range of costs that could be reduced (40–70%), although the costs of development, installation and transportation for the solar process should vary in this range to be competitive with the conventional process.

To conclude this section, the utilization of concentrated solar energy in the production of silicon-calcium is proposed in this manuscript. Solar energy arises as a suitable candidate because:

- high temperatures are required in the process (> 1700 °C);
- the process is energy intensive (> 10,000 kWh, Robiette, 1973);
- the production quantities are not excessively elevated (approximately 150,000 tons are produced worldwide, and around 15,000 tons per plant);
- the discontinuous operation is possible because the quantities produced daily in each plant are not excessively big, for instance, 40–50 t/day are produced in Chateau Feuillet (France). This way, operating in off-peak hours for electricity (night), when the energy is usually least expensive, is a common practice in the energy intensive industries if the production process/requirements allow it.

2. Materials and methods

Experiments were carried out in a 1.5 kW (maximum power) vertical axis solar furnace (Fig. 1) located in Odeillo (France) and belonging to the PROMES-CNRS (Procédés Matériaux et Énergie Solaire – Centre National de la Recherche Scientifique). The functioning of the vertical axis solar furnace can be summarized in that a solar tracking heliostat reflects the rays towards a 2.0 m in diameter parabolic concentrator, which makes converging sun radiation in a focal point of approximately 12–15 mm in diameter. In this way, incident radiation is concentrated a maximum of 15,000 times. The average incident radiation during the experiments varied in the range 722–841 W/m^2, with fluctuations in the own experiment that did not overcome ± 10%. The control of the power applied in each experiment was carried out with a venetian blind (shutter opening, which indicates the percentage of aperture of the venetian blind, 0 closed, 100 totally opened). Three sets of mixtures were prepared varying the proportion of silicon (25 wt.%, 50 wt.% and 75 wt.%) in the mixture calcium carbonate-silicon to know in what situation the best results were obtained. In Fig. 2 it is possible to locate the different compositions after the conversion of weight percentages into molar percentages, and see what temperatures would ensure the presence of liquid silicon-calcium. The obtaining of the silicon-calcium was performed using the method that in the Introduction was identified with the name *Method 2.1*, reduction of limestone with metallurgical silicon. Using limestone is less favorable than using lime because the calcium carbonate must be calcined into lime before being reduced with silicon to obtain the silicon-calcium. This way, if silicon-calcium is obtained using this method, it will be also synthesized using lime as starting material. Special atmosphere was not used during the experiments. Samples were located under a glass hood connected to a pump that led to a pressure inside of the glass chamber of 0.85 atm. This way, gases that were released during the experiments did not end in the parabolic concentrator. Despite the pump was

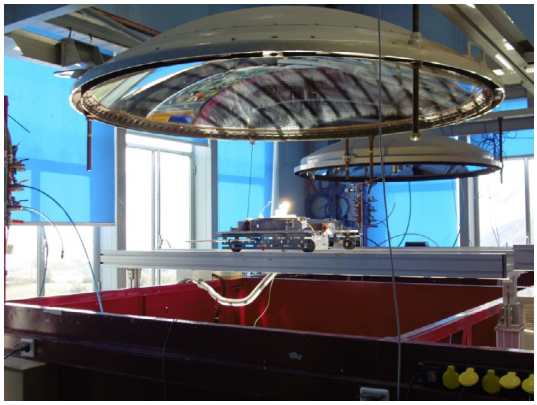

Fig. 1. Parabolic concentrator and sample located below the focal point (before the beginning of the process).

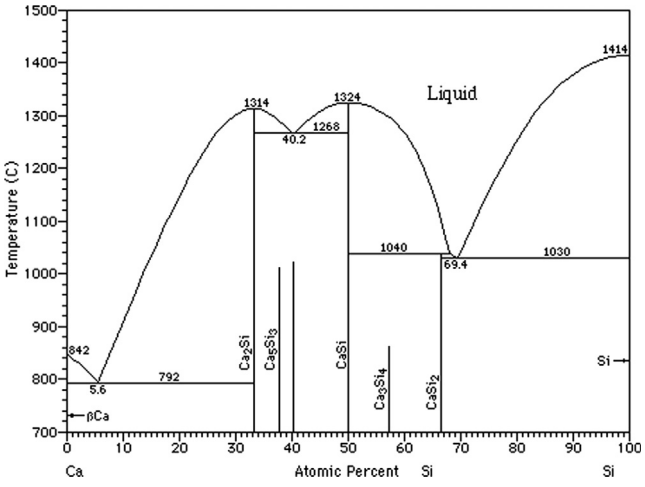

Fig. 2. Ca-Si binary diagram (TAPP 2.2 software).

connected before the experiments, there was not vacuum conditions during the experiments, and the atmosphere during the experiments was oxidizing, like the ambient atmosphere. This led to oxidation of the materials in the surface in contact with the beam, and it is assumed that this layer could protect the lower layers from the oxidation. It will be later seen that mass was only gained in three of the samples, concretely in those where the silicon content was bigger. Oxidation of silicon in the reaction layer to form silica is reasonable due to the reactions involved in the silicothermic process to obtain calcium, and this silica with the lime will form the silicates of the slag. It should be remembered that the reductant reagent used in the experiments was metallurgical quality silicon (99 wt.% Si); carbonaceous materials were not used to reduce the charge.

Calcium carbonate was analyzed using X-ray diffraction and X-ray fluorescence techniques. X-ray fluorescence was done with wavelength dispersive X-ray fluorescence spectrometer (Axios PANalytical) equipped with an Rh-anode x-ray tube with maximum power 4 kW. All samples were measured in vacuum with 15–50 eV energy resolution. For quantitative analysis of the spectra, the PANalytical standardless analysis package Omniam was used. X-ray diffraction measurements of powdered samples were conducted with Empyrean PANalytical diffractometer using Kα1 and Kα2 radiation from Cu anode. All measurements were performed with Bragg-Brentano setup at room temperature with the 0.006° step size at 5–90° 2θ scanning range and the 145 s of measurement time for each step. Data analysis and the peak profile fitting procedure were carried out using XPowder12 Ver. 01.02 (Database PDF2 (70–0.94)). Results for the calcium carbonate are collected in Table 1 and Fig. 3. It is not possible to see in Table 1 the presence of carbon due to the measurement conditions (measurement conditions of the fluorescence equipment did not detect carbon), but its presence can be checked in Fig. 3 (calcium carbonate, $CaCO_3$, is identified in X-ray diffraction analysis). Apart from calcium carbonate ($CaCO_3$), calcium oxide (II) (CaO) and calcium hydroxide ($Ca(OH)_2$) appear as other phases, although in smaller quantities.

Mixtures were loaded in crucibles of tabular alumina with the following dimensions: 55 mm in height, 30 mm in upper diameter, 25 mm in lower diameter and 3 mm in thickness of the crucible walls. The crucible was located below the focal point, which had approximately 15 mm in diameter. Temperatures were measured with a series of thermocouples, two of them located inside of the crucible, while the third one was located at an average height in the outer part of the crucible. Cromel-Alumel thermocouples (type K) were used. Maximum temperature that these thermocouples can register is 1382 °C, thus once overcame this temperature, they were burnt. Thermocouples were burnt in all experiments, consequently temperatures were higher than this temperature during the tests described in this paper. For that reason, this measurement cannot be used to offer a real knowledge of the temperature evolution, but it confirms that temperatures were higher than 1400 °C. It is possible to check in the Ca-Si diagram in Fig. 2 that the maximum temperature of the last solid phase in this diagram is 1414 °C (silicon melting point), above this temperature there is only liquid. This temperature was clearly reached in the experiments presented in this manuscript because both the thermocouples located inside of the crucible were burnt and liquid/molten phase was available during the experiments. Heating rate was of hundreds of degrees per second, while the cooling rate was of hundreds of degrees per minute. Fig. 4 shows the presence of molten phase in the crucibles during the experiments. Despite the presence of liquid phase in the crucible, the treated material was only observed in 12–20 mm in height. There was unreacted powdered material in the crucible after the treatment.

Table 1
Chemical composition of the calcium carbonate.

Compound	Mass percent (%)
Na_2O	0.047
MgO	0.611
Al_2O_3	0.334
SiO_2	0.748
P_2O_5	0.017
SO_3	0.343
K_2O	0.017
CaO	97.535
MnO	0.165
Fe_2O_3	0.111
SrO	0.049
Y_2O_3	0.003
Cl	0.021

Experimental conditions are collected in Table 2. All experiments lasted 12 min with different times at different values of rising powers to achieve a progressive heating: 2 min with 30 shutter opening (Power1); 3 min with 60 shutter opening (Power2); and 7 min with 85 shutter opening (Power3). A statistical analysis to see that experiments were performed under similar conditions was done (it is necessary taking into account the limited data that lead to high values of standard deviation and coefficient of variation, CV): the mean incident radiation was 755 W/m^2 (standard deviation: 38.2; CV: 0.05); regarding the values of power, the mean power 1 was 341 W (standard deviation: 16.2; CV: 0.05), power 2 was 679 W (standard deviation: 34.3; CV: 0.05) and power 3 was 970 W (standard deviation: 52; CV: 0.05). From the statistical results it is possible to deduce that there is not big heterogeneity/dispersion in the values of incident radiation and power. It is reasonable to say that experiments were performed under similar conditions. Only in the samples CaSi18 and CaSi19 the incident radiation took values slightly far from the mean value, and the power applied in this experiments was slightly higher than in the other cases. Once the sample was subjected to the above mentioned cycle of heating, the sample was removed from the solar beam and was air-cooled down to the room temperature.

Mass differences were calculated by difference between the weight of the final sample and the weight of the initial sample. In the case of the samples with: 25 wt.% Si, the mean mass loss was 2.5% (standard deviation: 1.2; CV: 0.5); 50 wt.% Si, the mean mass loss was −0.4% (standard deviation: 3.4; CV: 8.5); and, 75 wt.% Si, the mean mass loss was −1.5% (standard deviation: 1.6; CV: 1). It is possible to deduce from this statistical analysis that there is a great heterogeneity in the values of the mass differences in the three cases presented in Table 2. Despite the great heterogeneity in the results, it is seen that when the silicon is increased in the samples, the samples pass from losing mass to gain mass. This way, when using 25 wt.% Si, the mean mass loss was 2.5%, while when using 75 wt.% Si, the mean mass loss was −1.5% (mass was gained). The conclusion that can be deduced is that increasing silicon in the sample leads to more silicon available in the surface in contact with the atmosphere that can be oxidized (to form silica which neither reduces the lime nor reacts with the calcium to form the silicon-calcium). On the contrary, in the sample with 25 wt.% Si, more calcium carbonate is available in the sample, and in the surface would protect the rest of the sample from the oxidation, but above 900 °C calcium carbonate decomposes into calcium oxide (II) and carbon dioxide. Carbon dioxide leaves the sample as gas, and mass losses are produced as a result of the calcination process. The emissions of CO_2 (and projections of particles) associated to the calcination of the calcium carbonate can be observed in Fig. 5.

3. Results and discussion

Powders of the final samples taken from the zone affected by the solar radiation were analyzed using X-ray diffraction technique. There is not clear distinction between metal and slag because slag-forming elements were not added during the experiments (fluorspar). Conditions of the X-ray diffraction measurements of the powdered samples were indicated in Section 2. The X-ray diffraction patterns are showed in Figs. 6–8 (25 wt.% Si), Figs. 9–11 (50 wt.% Si) and

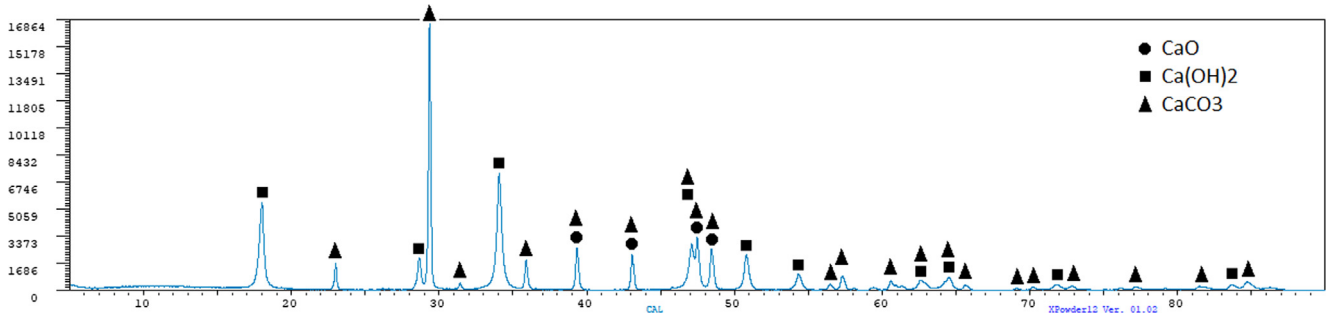

Fig. 3. X-ray diffraction pattern for the calcium carbonate (the same calcium carbonate was used in the experiments described in Fernández-González et al. (2018b)).

Fig. 4. Presence of molten phase in the crucibles during the experiments.

Table 2
Experimental conditions used in each test.

		Mass difference (%)	Incident radiation (W/m^2)	P1 (W)	P2 (W)	P3 (W)
25% Si	CaSi13	1.1	722	325	650	921
	CaSi14	3.6	723	336	651	933
	CaSi18	2.7	783	352	705	1010
50% Si	CaSi11	0.0	743	334	669	947
	CaSi12	−4.0	728	328	655	928
	CaSi17	2.8	767	345	690	989
75% Si	CaSi15	−1.4	739	333	665	953
	CaSi16	0.0	746	336	671	962
	CaSi19	−3.1	841	378	757	1085

Fig. 5. Emissions released during the experiments.

Figs. 12–14 (75 wt.% Si).

The main remark that can be deduced from the X-ray diffraction analysis is that calcium was detected in all samples. In this way, calcium is obtained via silicothermic reduction of the calcium oxide (II). This question leads to the following conclusions: calcium carbonate was calcined into calcium oxide (II) due to the heat supplied by the concentrated solar energy (calcination of the limestone takes place at temperatures above 900 °C); and the calcium oxide (II) is reduced with the silicon to form calcium. The controlling stage of the process is the calcination of the limestone. If calcium oxide (II) was not available to react with the silicon, there would not be calcium in the final sample. Calcium formed due to the silicothermic reduction of the calcium oxide (II) forms with the silicon the silicon-calcium alloy. Therefore, the process progresses according to the Method 2.1 presented in the Introduction section. $Ca_3Si_2O_7$ and $Ca_{10}O_{25}Si_6$ are also identified during the X-ray diffraction analysis. These two phases would be part of the slag. However, both phases were identified during the X-ray diffraction analysis, and this confirms that there is not proper separation metal-slag. Finally, it is possible to deduce from the X-ray diffraction analyses that the calcination and the silicothermic reduction did not progress to the bottom of the crucible because we identified $CaCO_3$, which indicates that the limestone was not completely calcined. This explains the existence of powders below the layer of densified and reacted material.

A quantitative analysis of the phases identified during the X-ray diffraction analysis was performed. Quantities were calculated using the program XPowder12 Ver. 01.02 without considering the presence of amorphous phases. Results of the quantitative analysis of the crystalline phases identified during the X-ray diffraction are collected in Table 3. Before the statistical analysis it is reasonable to confirm that there is a big dispersion in the results because the sample taken for the X-ray analysis was randomly taken from the final product, and the powders might come either from a region enriched in slag or from a region enriched in silicon or from a region enriched in mixture silicon-calcium. Apart from that, experiments were only repeated three times each set of them. SEM-EDX in Fig. 15 (EDX spectra are shown in Fig. 16) shows a micrograph of a sample where silicon-calcium, calcium silicate and silica are observed in the same region. The situation observed in Fig. 15 is the same that is observed in the other samples. A statistical analysis was performed considering only the silicon-calcium mixture for the quantitative analysis. In the case of the samples with: 25 wt.% Si, the mean Si was 36.5% (standard deviation: 16.5; CV: 0.45) and the mean Ca was 63.5% (standard deviation: 22.1; CV: 0.34); 50 wt.% Si, the mean Si was 47.1% (standard deviation: 38.2; CV: 0.8) and the mean Ca was 52.9% (standard deviation: 38.2; CV: 0.72); and, 75 wt.% Si, the mean Si was 47.7% (standard deviation: 17.4; CV: 0.37) and the mean Ca was 52.3% (standard deviation: 17.4; CV: 0.33). The statistical analysis indicates that there is a big heterogeneity/dispersion in the results, resulting from a limited number of experiments (the same was observed in the other statistical analyses). Thus, it is observed from the X-ray diffraction that silicon-calcium mixtures were detected but it is not possible to ensure that the analyses are representatives of the entire

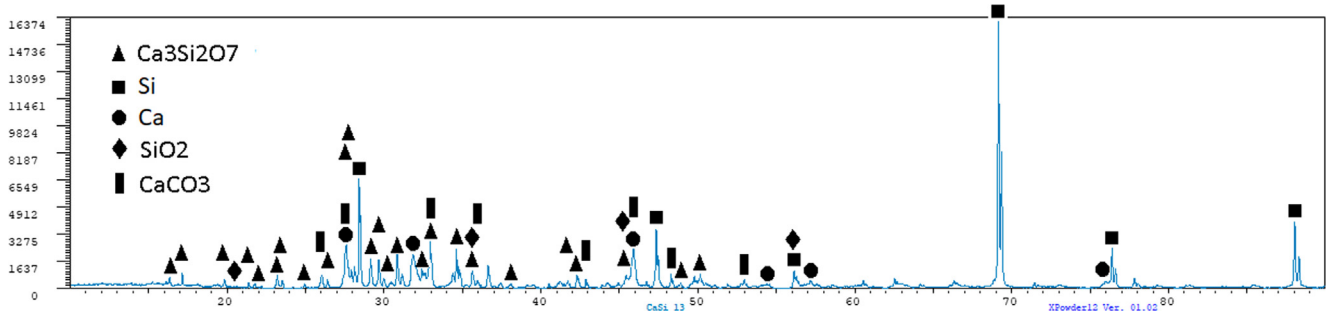

Fig. 6. X-ray diffraction pattern of the sample CaSi13.

sample. Increasing the number of experiments in each group, apart from achieving a proper separation metal-slag, to have a representative composition of the silicon-calcium obtained, is necessary. It is deduced from the statistical analysis that increasing the silicon percentage in the initial mixture would rise the silicon percentage in the final mixture. At the same time, increasing the silicon percentage in the initial mixture led to mass gains resulting from the oxidation of the silicon under the ambient atmosphere used in the experiments.

The solidification of the melt was analyzed using the Ca-Si phase diagram of the Fig. 2. Once silicon and calcium in liquid state were available, if the solidification would have progressed like equilibrium solidification, different calcium silicides should be found at the end of the solidification depending on the silicon percentage. However, mixtures silicon-calcium were detected at the end of the solidification. This way, the solidification progressed according to non-equilibrium solidification. A heterogeneous liquid formed by calcium, silicon (and the slag) was fast cooled down to the room temperature (air-cooling). Due to this fast cooling, there is not enough time for the formation of the equilibrium phases (calcium silicides). Furthermore, the treatment lasted only 12 min and, heating, calcination, silicothermic reduction of the lime and homogenization of the liquid must have taken place in this period of time. For future experiments, the duration of the treatment should be increased, and the cooling should be performed slower. This way, the obtaining of the calcium silicides could be attempted. Anyway, the objective of synthesizing silicon-calcium was satisfied.

The detection of the different phases identified in the X-ray diffraction analyses was done using SEM-EDX. Fig. 15 shows a micrograph of the sample CaSi11. This micrograph is representative of the situation that was observed in all samples: silicon-calcium mixture (phase of interest) mixed with the products of reaction, silica, coming either from the silicothermic process or from the oxidation of the silicon, and calcium silicates, which would form the slag. Table 4 provides the wt. % of the elements identified in the point analysis (Fig. 16 shows the EDX spectra). The aluminum detected in the point analysis has its origin in the impurities of the limestone; carbon in the samples was added before SEM-EDX analysis with the purpose of making the sample conductive.

Considering the point analysis (Table 4, Fig. 16), we can see the phases identified during the X-ray diffraction analysis: the point 1 represents the silicon-calcium mixture, in this case Ca-rich mixture; the point 2 represents the calcium silicates ($Ca_3Si_2O_7$ and $Ca_{10}O_{25}Si_6$); and, the point 3 is the silicon oxide (SiO_2), product either of the lime silicothermic process or the silicon oxidation with the ambient air.

High-calcium compounds and metallic calcium have low melting point, and particularly metallic calcium has low boiling point (1484 °C). Calcium might be volatilized at the temperatures involved in the concentrated solar energy process. This question could also remark the presence of calcium and justify the presence of bubble holes (see Fig. 17). The calcination of the calcium carbonate also generates gas, carbon dioxide, which might also produce bubble holes in the sample.

Resulting from the X-ray diffraction analyses and from the SEM-EDX it is possible to say that the process progressed as follows. First, calcium carbonate is calcined at around 900 °C to form lime (calcium oxide (II) and release carbon dioxide (before the calcination, several reactions of dehydration took place)). At the same time, silicon in contact with the atmosphere inside the glass chamber (oxidizing ambient atmosphere) oxidizes to form silica. Here it is possible to establish two situations: samples with low silicon (high calcium carbonate), where mass losses due to the calcination of the limestone were higher than the mass gains due to the oxidation of the silicon; or samples with high silicon (low calcium carbonate), where mass losses due to the calcination of the limestone were smaller than the mass gains due to the oxidation of the silicon. At this point it is possible to say that the controlling step for the process is the calcination of the limestone, if lime is not available, the silicothermic reduction of the calcium oxide cannot take place, and the silicon-calcium would not be formed. It is evident that lime is available in all experiments because calcium is identified at the end of the process. Once lime is available, silicon reduces the lime to produce calcium via silicothermic reduction. In this moment, calcium silicates (formed by reaction between the lime and the silica), silica, limestone (rests of unreacted material), silicon and calcium would be available, most of them in liquid state. Due to the oxidizing environment, there were risks of re-oxidation of the formed products. Apart from that, there was not proper separation metal-slag and, in this situation might have given zones with high calcium and low silicon, and vice versa. This way, different silicon-calcium mixtures (with different proportions of each constituent) could be obtained and the quantitative analysis of the

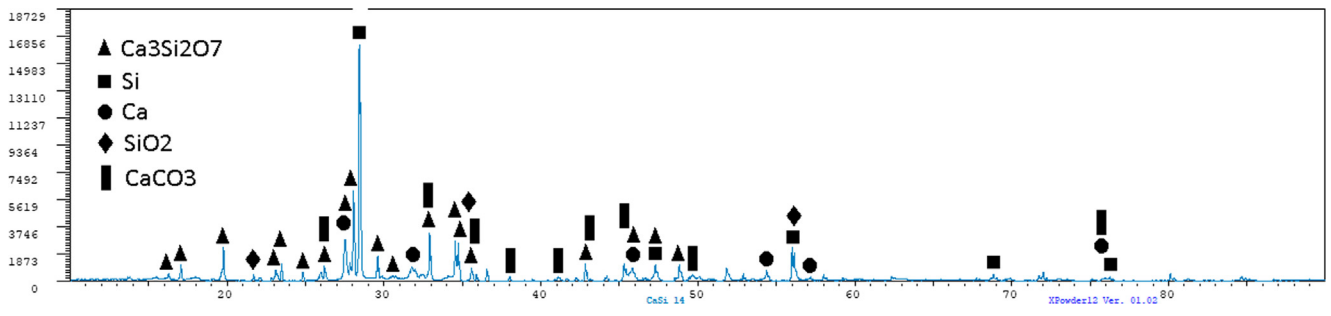

Fig. 7. X-ray diffraction pattern of the sample CaSi14.

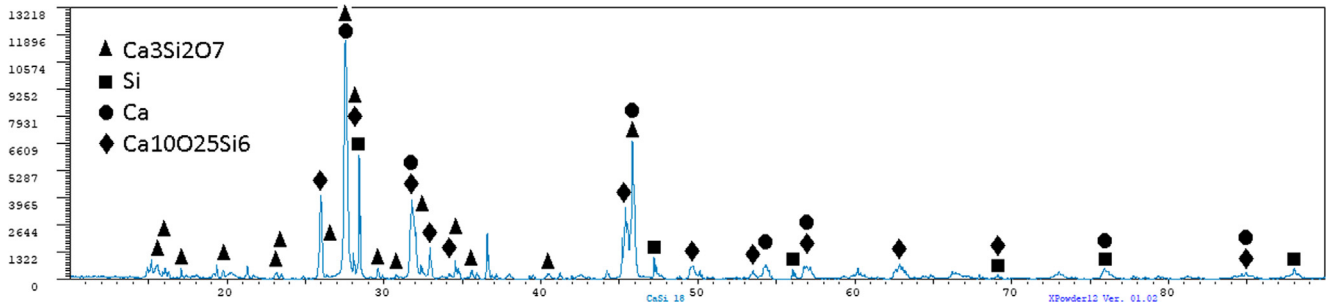

Fig. 8. X-ray diffraction pattern of the sample CaSi18.

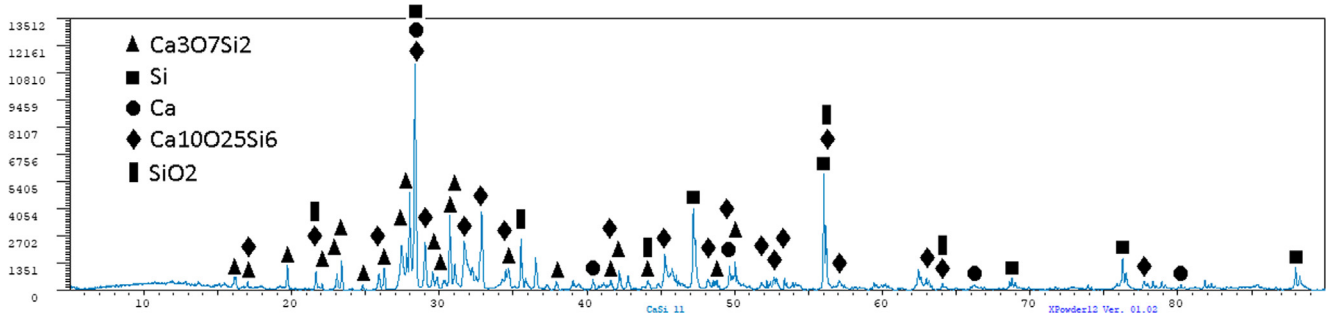

Fig. 9. X-ray diffraction pattern of the sample CaSi11.

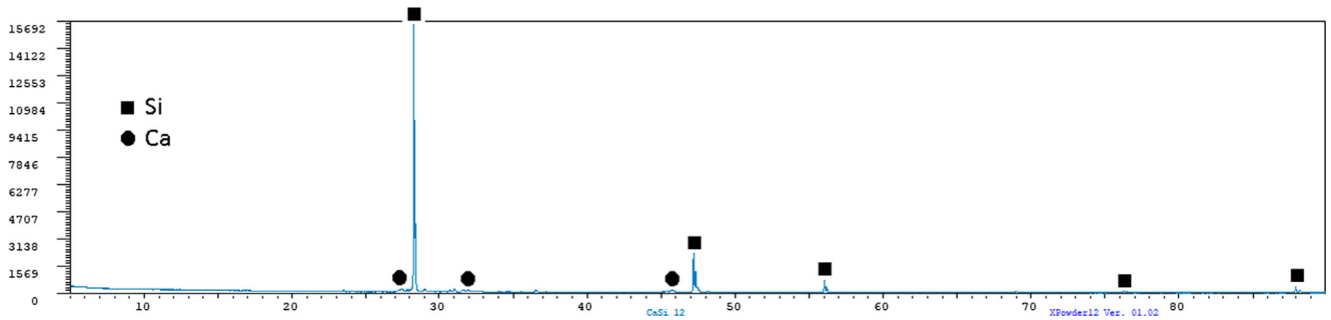

Fig. 10. X-ray diffraction pattern of the sample CaSi12.

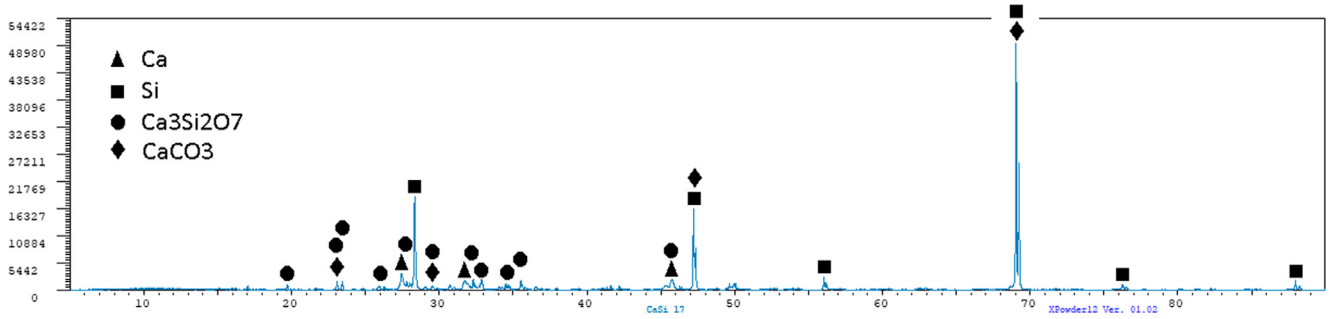

Fig. 11. X-ray diffraction pattern of the sample CaSi17.

phases identified during the X-ray diffraction analyses give different proportions of calcium and silicon in the mixture. The mixture was fast cooled down to the room temperature using air cooling. After that, we obtain the calcium-silicon mixtures detected in the X-ray diffraction and SEM-EDX analyses. If proper separation metal-slag would have been achieved, and the mixture had been in liquid state for longer times, both equilibrium calcium silicides and homogeneous (in percentage) silicon-calcium mixtures would have been obtained.

Several questions have arisen during the experiments that should be solved in future experiments:

- The separation metal slag. This question is fundamental, if there is not proper separation metal-slag, the process has no interest. In the industrial practice slag-forming elements are added (fluorspar) to improve the fluidity of the slag and, in this way, separate adequately the alloy from the slag.
- The volume of material treated during the experiments. This question is related with the power of the furnace used in the experiments (1.5 kW max., focal point of 12–15 mm in diameter) because powerful furnaces will allow increase the focal point dimensions, and thus the treated volume.

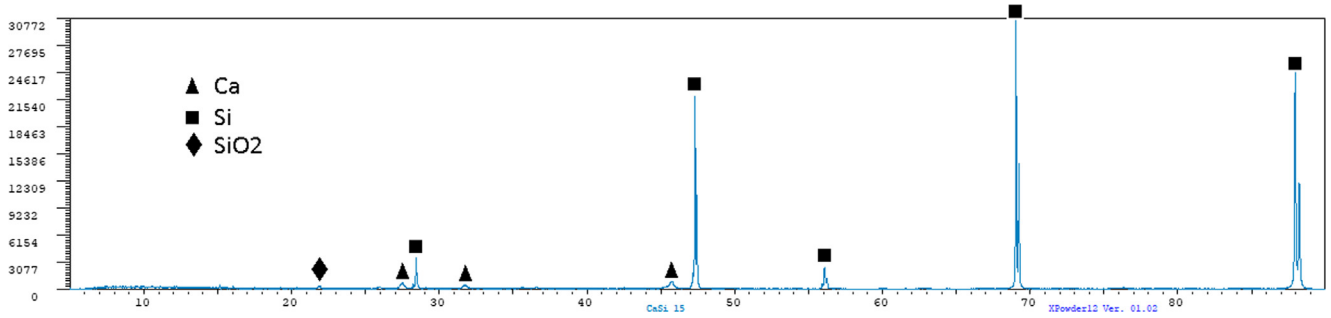

Fig. 12. X-ray diffraction pattern of the sample CaSi15.

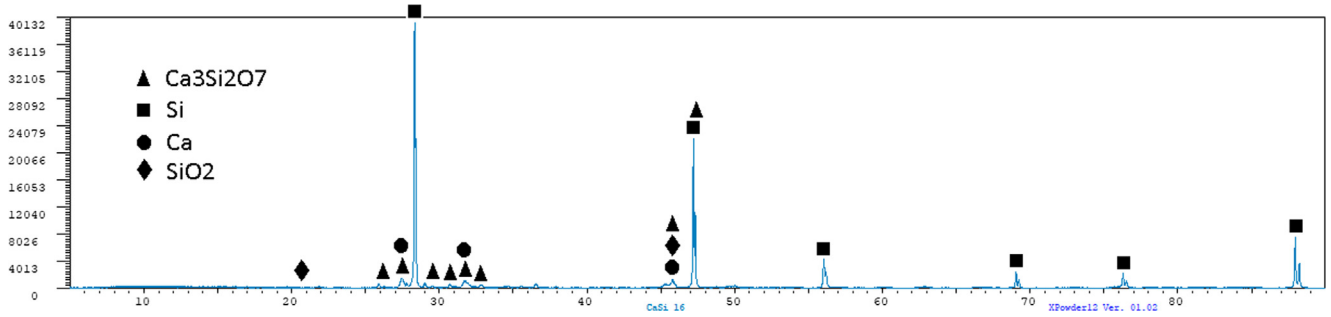

Fig. 13. X-ray diffraction pattern of the sample CaSi16.

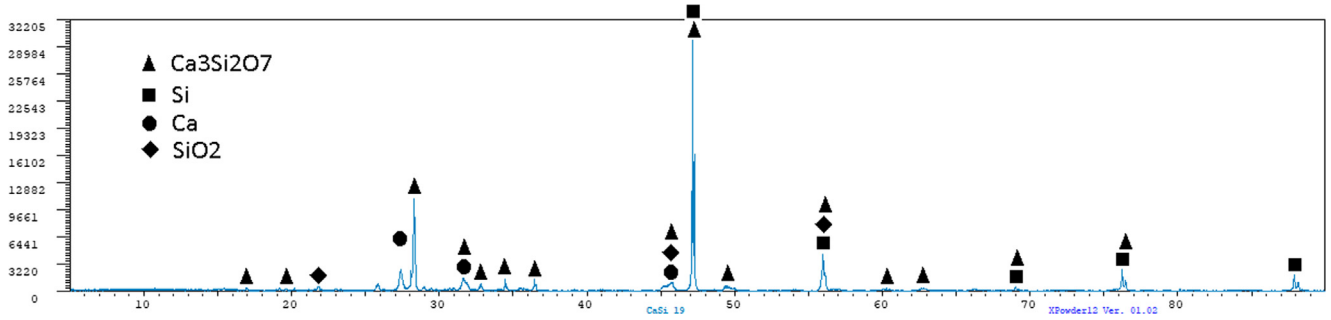

Fig. 14. X-ray diffraction pattern of the sample CaSi19.

Table 3
Quantitative analysis discounting the presence of amorphous phases.

	25% Si			50% Si			75% Si		
	CaSi13	CaSi14	CaSi18	CaSi11	CaSi12	CaSi17	CaSi15	CaSi16	CaSi19
Si	15.9 ± 0.9	34.0 ± 0.8	10.8 ± 1.4	7.3 ± 2.2	87.2 ± 0.1	28.6 ± 0.3	27.3 ± 0.4	48.0 ± 0.4	21.2 ± 0.4
Ca	30.0 ± 2.3	23.2 ± 2.5	59.4 ± 1.2	58.1 ± 1.1	12.8 ± 0.4	38.2 ± 0.8	38.7 ± 1.2	23.2 ± 1.2	40.6 ± 1.1
$Ca_3Si_2O_7$	36.4 ± 2.1	26.3 ± 2.5	7.2 ± 3.7	12.1 ± 3.3		24.3 ± 0.9		12.7 ± 1.3	12.3 ± 1.3
$Ca_{10}O_{25}Si_6$			22.6 ± 2.9	13.0 ± 3.3					
SiO_2	8.6 ± 2.8	9.0 ± 2.6		9.5 ± 3.4			34.0 ± 1.2	16.1 ± 1.2	25.9 ± 1.2
$CaCO_3$	9.1 ± 2.9	8.4 ± 2.7				8.9 ± 1.0			

– The duration of the treatment. Probably the duration of the treatment (12 min) was too short in our experiments, because the following processes must take place in this time: heating of the initial mixture, calcination of the limestone, reduction of the lime via silicothermic reduction and homogenization the liquid. Furthermore, the cooling should be slower if equilibrium solidification is aimed. Producing the lime in a separated stage could be more adequate due to the calcination of the limestone is the controlling step in our process.
– The oxidation and risks of re-oxidation. The utilization of a reductant atmosphere or at least a protective atmosphere should be required to minimize the oxidation of the initial silicon. If the silicon is oxidized, it will not reduce the calcium oxide (II) and will not form the silicon-calcium oxide.

Despite the problems observed during the experiments described in this manuscript, it was demonstrated that using concentrated solar energy it is possible to obtain silicon-calcium. This paper offers preliminary research about the utilization of solar energy in the synthesis of this alloy and, consequently, further research should be carried out to solve all the problems identified during the experiments presented in this manuscript. Anyway, in contrast with other metallurgical processes, silicon-calcium production plants handle quantities of product that do not make necessary operating 24 h every day, and they can take

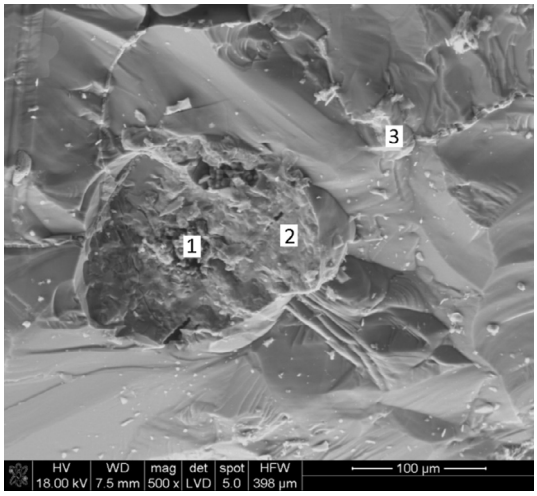

Fig. 15. SEM image of the sample CaSi11.

Table 4
Point analysis for the sample CaSi11.

Element (wt.%)	Point 1	Point 2	Point 3
O	2.79	8.56	28.66
Si	13.48	21.51	70.39
Ca	83.73	37.67	
C		29.79	28.66
Al		2.47	0.95

advantage of the off-peak hours when the electricity is less expensive (discontinuous operation is possible). Moreover, the production of not only silicon-calcium alloy, but also of other ferroalloys, is energy intensive whether it is compared with other metallurgical processes. For example, the production of steel requires 3000–4000 kWh per ton of steel, while 10,000–15,000 kWh are required per ton of silicon-calcium alloy. Additionally, carbon dioxide emissions might be reduced using the concentrated solar energy as it was indicated in Section 1, apart from all mentioned in that section about the potential reduction in

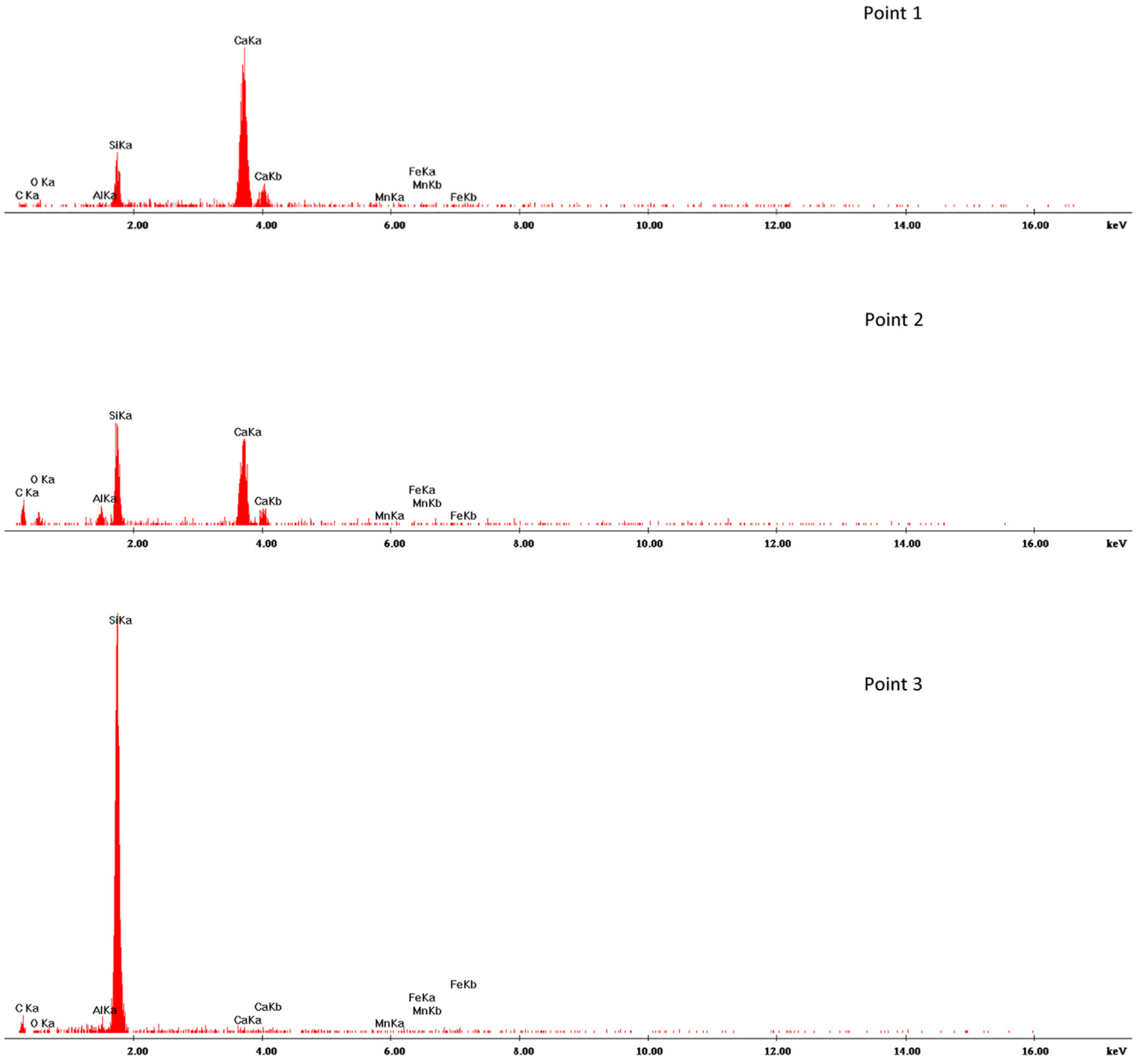

Fig. 16. EDX spectra: y-axis indicates the number of counts and x-axis the energy of the X-rays.

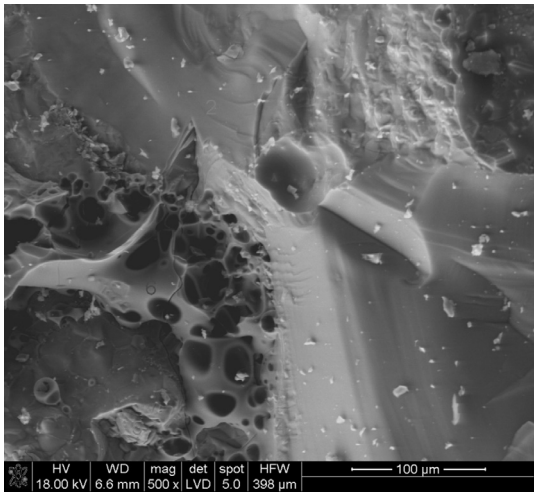

Fig. 17. Bubbles probably caused by the volatilization of the calcium.

costs. Thus, concentrated solar energy arises as a suitable candidate for the production of silicon-calcium alloy. In this paper it was demonstrated that it is possible to use solar energy in the production of silicon-calcium, although several questions should be further improved to increase the quantity and quality of the synthesized alloy.

4. Conclusions

In this paper the synthesis of silicon-calcium using concentrated solar energy was proposed. Results show that this process is really promising, because reductions in costs and environmental improvements might be achieved. Silicon-calcium mixtures were identified in all experiments using x-ray diffraction and SEM-EDX. Thus, the objective presented at the beginning of the process was satisfied. Silicon-calcium mixture was found mixed with calcium silicates ($Ca_3Si_2O_7$ and $Ca_{10}O_{25}Si_6$) and silica (SiO_2). This indicates that there is not a proper separation metal-slag. This question could be solved using slag-forming elements, fluxes and other elements that could increase the fluidity of the slag. Other of the problems observed during the experiments was the oxidation of silicon added to reduce the lime. This way, reductant or inert atmosphere should be also used to minimize/avoid the oxidation of the silicon. Ferrosilicon could be used instead of metallurgical silicon because this alloy is less expensive than the metallurgical silicon.

This paper offers preliminary research about the utilization of concentrated solar energy in the production of silicon-calcium. However, further research must be performed to increase the quantity and quality of silicon-calcium obtained during the process. Despite the problems indicated along the manuscript, concentrated solar energy arises as a suitable candidate in the production of silicon-calcium alloy because of: the high temperatures required in the process ($> 1700\,^{\circ}C$); the production quantities are not excessively elevated, approximately 150,000 tons are produced worldwide; the possibility of operating discontinuously because the quantities produced daily in each plant are not excessively big, around 40–50 tons daily; and, the possibility of operating in off-peak hours for electricity (night), when the energy is usually least expensive.

Acknowledgements

Financial support by the Access to Research Infrastructures activity in the 7th Framework Program of the EU (SFERA 2 Grant Agreement n. 312643) is gratefully acknowledged and the use of the facilities and its researchers/technology experts. Project SOLMETBY (P1701250238), Investigation and evaluation of solar energy as energy source in the treatment of metallurgical by-products.

This research was supported by the Spanish Ministry of Education, Culture, and Sports via an FPU (Formación del Profesorado Universitario) grant to Daniel Fernández González (FPU014/02436).

References

Ballester, A., Verdeja, L.F., Sancho, J.P., 2003. Metalurgia Extractiva. Volumen 1: Fundamentos, first ed. Síntesis, Madrid.

Fernández, D., Ordiales, M., Sancho, J., Verdeja, L.F., 2015. Posibilidades de la lógica difusa en operaciones y procesos de la metalurgia primaria. In: Spain Minergy Congress 2015, Gijón/Xixón, Asturias, Spain, June 15–19, 2015.

Fernández-González, D., Ruiz-Bustinza, I., González-Gasca, C., Piñuela-Noval, J., Mochón-Castaños, J., Sancho-Gorostiaga, J., Verdeja, L.F., 2018a. Concentrated solar energy applications in materials science and metallurgy. Sol. Energy 170, 520–540.

Fernández-González, D., Prazuch, J., Ruiz-Bustinza, I., González-Gasca, C., Piñuela-Noval, J., Verdeja, L.F., 2018b. Solar synthesis of calcium aluminates. Sol. Energy 171, 658–666.

Fernández-González, D., Prazuch, J., Ruiz-Bustinza, I., González-Gasca, C., Piñuela-Noval, J., Verdeja, L.F., 2018c. Iron metallurgy via concentrated solar energy. Metals-Basel 8, 873.

Fernández-González, D., Prazuch, J., Ruiz-Bustinza, I., González-Gasca, C., Piñuela-Noval, J., Verdeja, L.F., 2019. The treatment of Basic Oxygen Furnace (BOF) slag with concentrated solar energy. Sol. Energy 180, 372–382.

Flamant, G., Hernández, D., Traverse, J., 1980. Experimental aspects of the thermochemical conversion of solar energy; Decarbonation of $CaCO_3$. Sol. Energy 24, 385–395.

Flamant, G., Ferriere, A., Laplaze, D., Monty, D., 1999. Solar processing of materials: opportunities and new frontiers. Sol. Energy 66, 117–132.

Flamant, G., Kurtcouglu, V., Murray, J., Steinfeld, A., 2006. Purification of metallurgical grade silicon by a solar process. Sol. Energy Mater. Sol. C. 90, 2099–2106.

Imhof, A., 1997. Decomposition of limestone in a solar reactor. Renew. Energy 10, 239–246.

Loutzenhiser, P.G., Tuerk, O., Steinfeld, A., 2010. Production of Si by vacuum carbothermal reduction of SiO_2 using concentrated solar energy. JOM J. Min. Met. Mat. S. 62, 49–54.

Meier, A., Bonaldi, E., Cella, G.M., Lipinski, W., Wuillemin, D., Palumbo, R., 2004. Design and experimental investigation of a horizontal rotary reactor for the solar thermal production of lime. Energy. 29, 811–821.

Meier, A., Gremaud, N., Steinfeld, A., 2005a. Economic evaluation of the industrial solar production of lime. Energy Convers. Manage. 46, 905–926.

Meier, A., Bonaldi, E., Cella, G.M., Lipinski, W., 2005b. Multitube rotary kiln for the industrial production of lime. J. Sol. Energy-T. ASME. 127, 386–395.

Meier, A., Bonaldi, E., Cella, G.M., Lipinski, W., Wuilleimin, D., 2006. Solar chemical reactor technology for industrial production of lime. Sol. Energy 80, 1355–1362.

Mochón, J., Ruiz-Bustinza, I., Vázquez, A., Fernández, D., Ayala, J.M., Barbés, M.F., Verdeja, L.F., 2014. Transformations in the iron-manganese-oxygen-carbon system resulted from treatment of solar energy with high concentration. Steel Res. Int. 85, 1469–1476.

Monsen, B.E., Lindstad, T., Tuset, J.K., 1998. CO2 emissions from the production of ferrosilicon and silicon metal in Norway. In: Electric Furnace Conference Proceedings, Special Arcs, Emission Control Session, New Orleans, USA, November 1998, pp. 371–378.

Murray, J.P., Flamant, G., Roos, C.J., 2006. Silicon and solar-grade silicon production by solar dissociation of Si_3N_4. Sol. Energy 80, 1349–1354.

Pero-Sanz, J.A., 2004. Aceros: Metalurgia Física, Selección y Diseño, first ed. CIE Inversiones Editoriales Dossat-2000, Madrid.

Pero-Sanz, J.A., Fernández-González, D., Verdeja, L.F., 2018. Physical Metallurgy of Cast Irons, first ed. Springer, Cham.

Robiette, A.G.E., 1973. Electric Smelting Process, first ed. John Wiley and Sons, New York.

Rodero, J.I., Sancho-Gorostiaga, J., Ordiales, M., Fernández, D., Mochón, J., Ruiz-Bustinza, I., Fuentes, A., Verdeja, L.F., 2015. Blast furnace and metallurgical coke's reactivity and its determination by thermal gravimetric analysis. Ironmak. Steelmak. 42, 618–625.

Ruiz-Bustinza, I., Cañadas, I., Rodríguez, J., Mochón, J., Verdeja, L.F., García-Carcedo, F., Vázquez, A., 2013. Magnetite production from steel wastes with concentrated solar energy. Steel Res. Int. 84, 207–217.

Sancho, J.P., Verdeja, L.F., Ballester, A., 2003. Metalurgia Extractiva. Volumen 2: Procesos de Obtención, first ed. Síntesis, Madrid.

Tanstad, M., 2013. Ferrosilicon and silicon technology. In: Gasik, M. (Ed.), Handbook of Ferroalloys. Theory and Technology. Butterworth-Heinemann (Elsevier), Oxford, pp. 179–219.

TAPP. Version 2.2. ES Microware Inc., Wade Court, Hamilton, OH.